BIOCHEMISTRY
including biophysical chemistry & molecular biology

ARTICLE

pubs.acs.org/biochemistry

1-Palmitoyl-2-(9′-oxononanoyl)-*sn*-glycero-3-phosphocholine, an Oxidized Phospholipid, Accelerates Finnish Type Familial Gelsolin Amyloidosis in Vitro

Ajay K. Mahalka,[†] C. Peter J. Maury,[‡] and Paavo K. J. Kinnunen*[,†]

[†]Helsinki Biophysics and Biomembrane Group, Department of Biomedical Engineering and Computational Science, Aalto University, Espoo, Finland

[‡]Department of Medicine, University of Helsinki, Helsinki, Finland

Supporting Information

ABSTRACT: Finnish type familial amyloidosis (FAF) is a neurodegenerative disease, which involves the deposition of D187N or -Y mutant gelsolin fragments as amyloid in various tissues, accompanied by dermatologic, neurologic, and ophthalmologic disorders. Like the other amyloid diseases, FAF is associated with oxidative stress. The latter results in an extensive chemical modification of biomolecules, such as the formation of a myriad of phospholipids with oxidatively modified acyl chains containing various functional groups. Here we demonstrate that 1-palmitoyl-2-(9′-oxononanoyl)-*sn*-glycero-3-phosphocholine (PoxnoPC), a zwitterionic oxidized phospholipid bearing an aldehyde moiety at the end of its truncated *sn*-2 acyl chain, accelerates amyloidogenesis of $FtG_{179-194}$ (i.e., the core amyloidogenic segment of residues 179−194 of FAF gelsolin) as revealed by thioflavin T (ThT) fluorescence and electron microscopy. These techniques and Trp fluorescence show that the accelerated conversion of $FtG_{179-194}$ into amyloid fibrils consists of distinct consecutive phases. PoxnoPC at a close to critical micelle concentration (∼22.5 μM) causes a maximal increase in ThT fluorescence and the K_{app} for fibril formation. The rates of fibril elongation and nucleation were proportional to PoxnoPC concentration, while the rates of nucleation were different below and above the critical micelle concentration. Our data also suggest an initial rapid formation of a 1:1 complex by PoxnoPC and $FtG_{179-194}$. The latter could involve a transient Schiff base and reside at the membrane hydrocarbon−water interface in the proximity of the phosphocholine headgroup. Subsequently, these profibrils insert into a more hydrophobic milieu and undergo a slow structural transition and assemble into amyloid fibers. Different phases can be expected when proteins aggregate on the phospholipid membrane surfaces, underlying the importance of a detailed kinetic analysis to fully understand the effects of oxidized phospholipids on amyloidogenesis. This study represents the first comprehensive analysis of the kinetics and mechanisms of amyloid formation in the presence of an oxidized phospholipid.

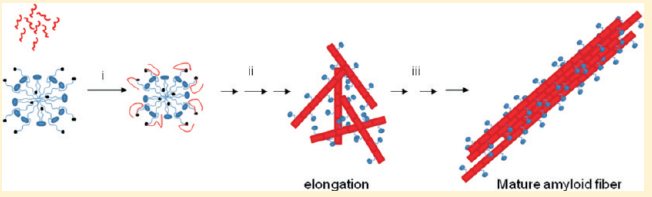

Finnish type familial amyloidosis (FAF) is a globally distributed autosomal, dominantly inherited neurodegenerative disease, originally reported in southeastern Finland[1] and later in several other European countries, North America,[1] and Japan.[2] FAF is characterized by an extensive deposition of D187N or -Y mutant gelsolin fragments as amyloid in various tissues, accompanied by dermatologic, neurologic, and ophthalmologic disorders in the third or fourth decade of life, causing cutis laxa, cranial neuropathy, and corneal lattice dystrophy.[3−9]

Gelsolin is a multifunctional[10] hexameric protein of homologous domains, each consisting of five-strand β-sheets sandwiched between two α-helices.[11] It regulates actin assembly through nucleation, capping, and severing, these functions being further controlled by Ca^{2+} and phosphoinositide binding.[12,13] Two forms of gelsolin are generated by alternative splicing,[14] an intracellular 81 kDa protein and a secreted 83 kDa protein. The former regulates the motility and architecture of cells,[12] whereas the latter removes actin filaments from the bloodstream, reducing the viscosity of the blood.[15] Conformational alterations within domain 2 of gelsolin due to the mutation of Asp-187 to Asn or Tyr in FAF cause a loss of Ca^{2+} binding that further renders the mutant gelsolin susceptible to furin and matrix metalloprotease type 1-catalyzed aberrant proteolysis,[16,17] generating an amyloidogenic precursor that deposits as amyloid plaque with the characteristic cross-β structure.[18] While both splice variants may contain the D187N or -Y mutation, only the secreted 83 kDa gelsolin is associated with amyloidosis in FAF.[19]

In aerobic organisms, the leakage of partially reduced oxygen from mitochondrial respiration represents the main source of the so-called reactive oxygen species (ROS), which are also generated by activated leukocytes as well as in various tissue specific enzymatic reactions, at sites of infection and inflammation in particular.[20] To defend against their cytotoxic effects, cells detoxify ROS through small molecule antioxidants and ROS-scavenging enzymes such as superoxide dismutases, catalases, and glutathione peroxidases. Depletion of the intracellular antioxidant pool together

Received: February 9, 2011
Revised: May 5, 2011
Published: May 05, 2011

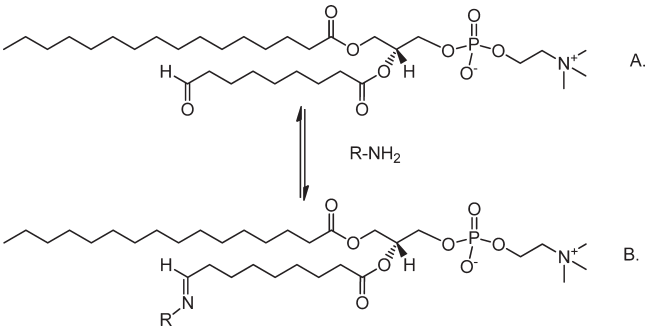

Figure 1. PoxnoPC (A) is formed upon peroxidation of polyunsaturated phospholipids such as 1-palmitoyl-2-linoleoyl-PC by reactive oxygen species (ROS). (B) Schiff base can be formed upon the reaction of the aldehyde moiety of PoxnoPC with an NH_2 moiety of a peptide (R).

with the inability to repair oxidative damage to DNA, proteins, and lipids under oxidative stress has been implicated in the pathogenesis of a number of diseases as well as aging.[21,22] Along these lines, there is evidence of elevated oxidative stress being associated with all forms of amyloid diseases, including FAF.[10,23]

The biophysical properties of phospholipid membranes undergo drastic changes upon the ROS-induced formation of a myriad of phospholipid derivatives with oxidatively polyunsaturated modified acyl chains containing a number of polar functional groups.[24] This is particularly relevant to cells such as neurons with a high content of polyunsaturated fatty acids, yielding upon peroxidation highly reactive aldehydes.[25] Besides being cytotoxic as such,[26] these aldehydes can covalently modify proteins and potentially alter their normal function.[27,28] Several converging lines of evidence suggest that interactions with lipid membranes promote various precursors to adopt partially folded aggregation-prone states involved in the assembly of amyloid fibrils.[24] Moreover, several lines of evidence have converged to show that amyloid cytotoxicity results from the permeabilization of the cellular membrane lipid bilayers (see refs 24 and 29 for recent reviews). Recent studies have demonstrated that oxidatively modified lipids can accelerate the formation of amyloid fibrils by Alzheimer's β-peptide and islet-associated polypeptide.[22,30−32] Oxidatively modified phospholipids such as 1-palmitoyl-2-(9′-oxononanoyl)-*sn*-glycero-3-phosphocholine (PoxnoPC), a zwitterionic phosphatidylcholine bearing an aldehyde group at the end of its truncated *sn*-2 acyl chain (Figure 1), also represent potential molecular targets for amyloidogenic host defense peptides, such as LL-37,[27] most likely involving Schiff base formation.

The amyloidogenic core is believed to be a critical determinant of the initiation of amyloid formation by the other fragments. Short peptide fibrils share the backbone structural properties of those derived from full-length proteins, and knowledge of the mechanisms of peptide fibrillation in the presence of, for instance, oxidized lipids thus serves as a foundation for understanding the aggregation of larger proteins. Accordingly, we studied the behavior of the core peptide in the presence of the indicated lipids, thus providing a simple and well-defined approach, yielding unambiguous data. In this work, we studied the influence of a number of different lipids, including PoxnoPC, on the formation of fibrils by the 16-residue peptide $FtG_{179-194}$ (i.e., segment of residues 179−194 of FAF gelsolin), which contains the D187N mutation and was shown to represent the amyloidogenic core of gelsolin[33] in FAF. Thioflavin T (ThT) and tryptophan fluorescence were used to monitor the time course of fibril formation,[34] which was also verified by electron microscopy. Notably, of the lipids studied, only PoxnoPC promotes the formation of fibrils by $FtG_{179-194}$ (D187N) at pH 7.0, and in 150 mM NaCl, in contrast to the lack of fibril formation by the corresponding wild type peptide $wtG_{179-194}$ under all conditions. To the best of our knowledge, this is the first demonstration of augmented amyloid formation by the amyloidogenic D187N core peptide of gelsolin in the presence of a lipid membrane under physiologically relevant conditions in vitro.

MATERIALS AND METHODS

Materials. 1-Palmitoyl-2-(9′-oxononanoyl)-*sn*-glycero-3-phosphocholine (PoxnoPC), 1-palmitoyl-2-azelaoyl-*sn*-glycero-3-phosphocholine (PazePC), 1-palmitoyl-2-oleoyl-*sn*-glycero-3-phosphocholine (POPC), and 1-palmitoyl-2-oleoyl-*sn*-glycero-3-phospho-*rac*-glycerol (POPG) were from Avanti Polar Lipids (Alabaster, AL). Acrylamide, cholesterol, ethylenediaminetetraacetic acid (EDTA), NaCl, *N*-(2-hydroxyethyl)piperazine-*N*′-2-ethanesulfonic acid (Hepes), and thioflavin T (ThT) were from Sigma, and sphingosine was from Matreya (Pleasant Gap, PA). The purity of these lipids was checked by thin layer chromatography on silicic acid-coated plates (Merck, Darmstadt, Germany), using a chloroform/methanol/water/ammonia mixture (65:20:-2:2, v/v) as the eluent. Examination of the plates after iodine staining revealed no impurities. Concentrations of the phospholipid stock solutions in chloroform were determined gravimetrically with a high-precision electrobalance (Cahn Instruments, Cerritos, CA), as described previously.[35]

Stock solutions (500 μM) of synthetic wild type $gelsolin_{179-194}$ ($wtG_{179-194}$, H_2N-SWESFNNGDCFILDLG-$CONH_2$) and Finnish mutant type D187N $gelsolin_{179-194}$ ($FtG_{179-194}$, H_2N-SWESFNNGNCFILDLG-$CONH_2$) fragments (Genscript Corp., Piscataway, NJ) with a high-performance liquid chromatography (HPLC) purity of >95% were made in 90% DMSO.

Preparation of Large Unilamellar Vesicles (LUVs). Appropriate amounts of the lipid stock solutions were mixed in chloroform, yielding the desired compositions. The solvent was removed under a stream of nitrogen, and the lipid residue was subsequently maintained under reduced pressure for at least 2 h. The dry lipids were hydrated at room temperature in 20 mM Hepes, 0.1 mM EDTA, and 150 mM NaCl (pH 7.0). To ensure efficient dispersion, we placed the solutions of neat PoxnoPC in a bath sonicator for 20 min, to obtain optically clear solutions. During this procedure, the samples were vortexed several times. Large unilamellar vesicles composed of POPC and Poxn oPC (X = 0.2) were prepared essentially as described above, except without sonication and with subjection of the hydrated lipid solution to 19 passes through a 100 nm pore size polycarbonate filter (Nucleopore, Pleasanton, CA) using a LiposoFast small volume homogenizer (Avestin). Measurements by dynamic light scattering confirmed an average diameter of approximate 100 nm for the phospholipid composition described above (Volinsky et al., manuscript in preparation).

ThT Fluorescence Assay. The kinetics of formation of fibrils by $wtG_{179-194}$ and $FtG_{179-194}$ fragments in the absence or presence of varying concentrations of PoxnoPC as such or POPC/PoxnoPC mixed liposomes were monitored by fluorescence spectroscopy for 50 μM ThT in a total volume of 200 μL of 20 mM Hepes, 0.1 mM EDTA, and 150 mM NaCl (pH 7.0). The reactants were mixed in an Eppendorf tube, and 200 μL aliquots

of these solutions were transferred into 96-well plates (black plastic with clear glass bottom, Greiner Bio-One, Frickenhausen, Germany).

The plates were subsequently sealed and loaded into a fluorescence microplate reader (SPECTRAFluor Plus, Tecan GmbH, Salzburg, Austria), equipped with 430 nm excitation (35 nm bandpass) and 485 nm emission (10 nm bandpass) filters. Use of transparent plates with a thin glass bottom allowed us to utilize these samples for both the ThT assay (bottom illumination mode) and epifluorescence microscopy to monitor aggregate morphology. ThT fluorescence was monitored over time at 27 °C, and the data from wells were corrected for baseline, normalized, and plotted as fluorescence intensity (arbitrary units) versus time.

Kinetics of Fibril Formation. The kinetics of fibril formation can be described by sigmoidal curves with an initial lag phase, with a very slow change in ThT fluorescence intensity, a subsequent growth phase with steeply increasing ThT emission, and a final equilibrium in which ThT fluorescence reaches a plateau, indicating the end of fibril formation. ThT fluorescence data were plotted as a function of time and fitted as described previously:[36]

$$I(t) = I_0 + m_0 t + \frac{I_\infty + m_\infty t}{1 + e^{-\left(\frac{t - t_{1/2}}{\tau}\right)}} \quad (1)$$

where $I(t)$ is fluorescence intensity, t is the time, $t_{1/2}$ is the time to reach 50% maximal fluorescence, and $I_0 + m_0 t$ and $I_\infty + m_\infty t$ represent the initial baseline corresponding to the induction period and the final plateau, respectively. The apparent rate constant, K_{app}, for the growth of fibrils is $1/\tau$, and the lag time is given by $x_o - 2\tau$. Importantly, while eq 1 is unrelated to the underlying molecular events, it provides a convenient method for comparing the kinetics of fibrillation.

Trp Fluorescence Spectroscopy. Alterations in the microenvironment of W180 upon the binding of $FtG_{179-194}$ to PoxnoPC were monitored by fluorescence spectroscopy.[37] Aliquots of 6.25 μM PoxnoPC dispersed in buffer (below) were added to a solution of $FtG_{179-194}$ (final concentration of 20 μM) in 20 mM Hepes, 0.1 mM EDTA, and 150 mM NaCl (pH 7.0), maintained at 25 °C with continuous stirring in a total volume of 1.8 mL. Approximately 1 min after each addition of PoxnoPC, fluorescence spectra for Trp were recorded with a Perkin-Elmer LS 50B spectrometer using 1 cm path length quartz cuvettes with both emission and excitation bandpasses set at 5 nm, with excitation at 290 nm and emission recorded from 308 to 450 nm, averaging five scans. Spectra were corrected for the contribution of light scattering in the presence of vesicles, and data are shown as a function of the lipid:peptide molar ratio. When indicated, W180 spectra were also recorded as a function of time at a constant lipid:peptide molar ratio.

Acrylamide is a water-soluble collisional quencher of Trp fluorescence and as a polar molecule does not penetrate into the nonpolar regions of either proteins or lipid bilayers.[38] Consequently, the extent of Trp quenching by acrylamide is a measure of the exposure of Trp to the aqueous phase and depends on the protein conformation and the mode of association of the peptide with lipids. Aliquots of a 3.0 M solution of acrylamide were added to a 20 μM $FtG_{179-194}$ solution in the absence or presence of PoxnoPC at the indicated peptide:lipid molar ratios, and spectra were recorded as described above. Three scans were averaged, and the values obtained were corrected for dilution, scattering, and the inner filter effect. The data were analyzed according to the Stern–Volmer equation:[39]

$$F_0/F = 1 + K_{sv}[Q] \quad (2)$$

where F_0 and F are the fluorescence intensities in the absence and presence of the quencher (Q), respectively, and K_{sv} is the Stern–Volmer quenching constant, providing in this case a measure for the access of acrylamide to W180.

Transmission Electron Microscopy. Assessment of the formation of fibrils by EM was accomplished for 3 μL samples placed on a 200-mesh copper grid covered by carbon-stabilized Formvar film. After 1 min, excess fluid was removed, and the grid was then negatively stained with 2% uranyl acetate in water. After 30 s, excess fluid was removed from the grid. Samples were viewed with an FEI Tecnai F12 (Philips Electron Optics, Eindhoven, The Netherlands) electron microscope operated at 80 kV. Films were digitized on a Gatan Multiscan 794 1K × 1K CCD camera (Gatan Inc., Pleasanton, CA).

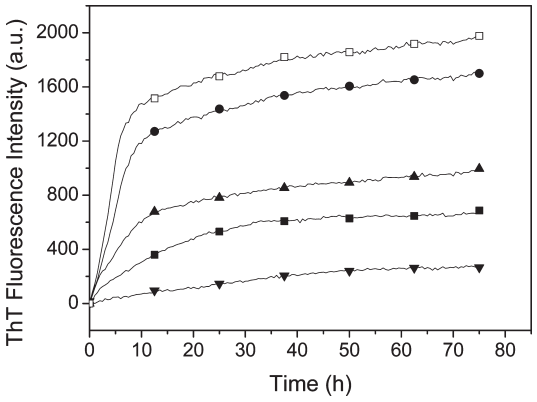

Figure 2. Kinetics of fibril formation by 5 (▼), 10 (■), 15 (▲), 20 (●), and 25 μM $FtG_{179-194}$ (□) monitored by the enhancement of ThT fluorescence. The measurements were continuous.

RESULTS

PoxnoPC Accelerates the Fibrillation of $FtG_{179-194}$. The fluorescent dye thioflavin T (ThT) binds to amyloid protofibrils and fibrils, resulting in a large increase in its quantum yield together with a change in the maximal emission wavelength.[40] ThT fluorescence enhancement is now widely used to monitor the extent of conversion of proteins into amyloid fibrils. We studied the fibrillation of $wtG_{179-194}$ and $FtG_{179-194}$ by ThT fluorescence in the presence of varying concentrations of different lipids and their mixtures in 20 mM Hepes, 0.1 mM EDTA, and 150 mM NaCl (pH 7.0). As expected, $FtG_{179-194}$ was amyloidogenic (Figure 2), whereas $wtG_{179-194}$ was nonamyloidogenic under all conditions (Figure S1 of the Supporting Information), emphasizing the role of Asp-187 as a gatekeeping negatively charged residue, preventing most likely due to electrostatic repulsion the proximity and alignment of gelsolin molecules required for the nucleation of amyloid fibril formation. Of the lipid compositions investigated, binary mixtures of POPC with POPG ($X = 0.2$), PazePC ($X = 0.2$), sphingosine ($X = 0.2$), or cholesterol ($X = 0.2$) had no detectable effect on the kinetics of $FtG_{179-194}$ fibrillation within a 200 h period, as judged by the lack of a significant increase in ThT fluorescence (data not shown). However, PoxnoPC, a zwitterionic oxidized phospholipid bearing

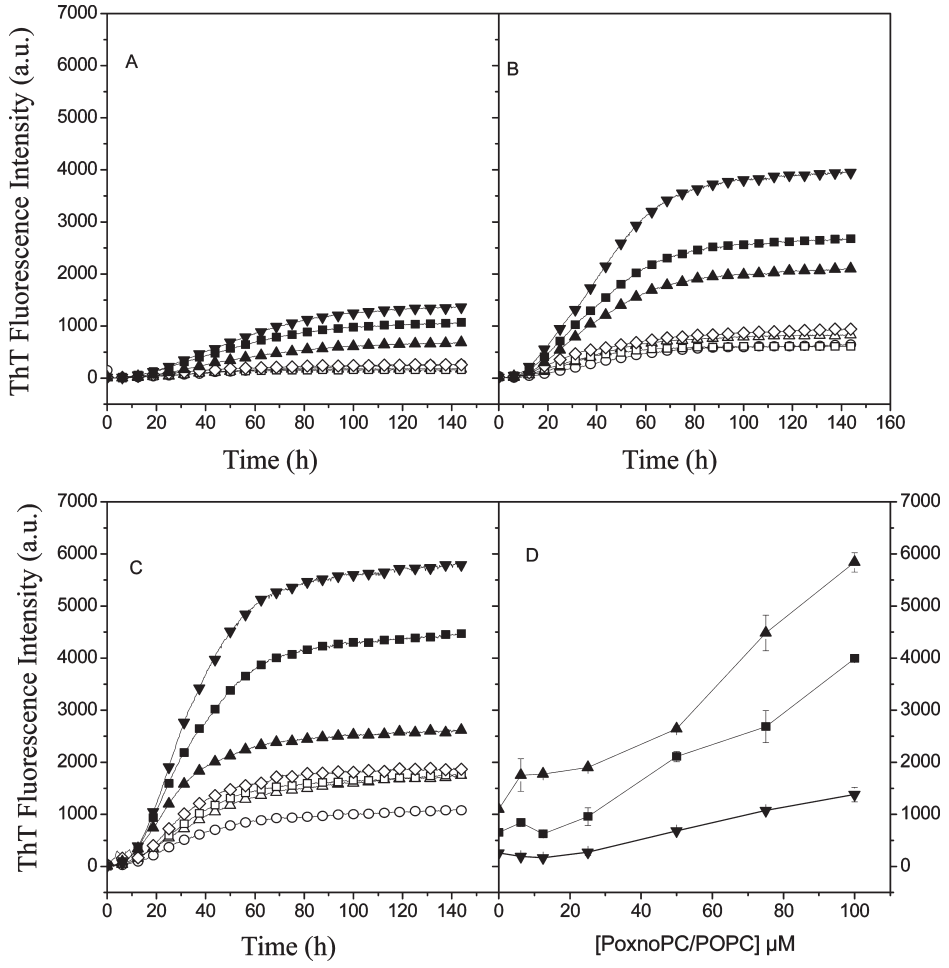

Figure 3. Kinetics of fibril formation by 5 (A), 10 (B), and 15 μM (C) $FtG_{179-194}$ in the presence of 0 (○), 6.25 (△), 12.5 (□), 25 (◇), 50 (▲), 75 (■), and 100 μM (▼) POPC/PoxnoPC ($X_{PoxnoPC}$ = 0.2) liposomes in a total volume of 200 μL of 50 μM ThT in 20 mM Hepes, 0.1 mM EDTA, and 150 mM NaCl (pH 7.0), measured at 27 °C without agitation or stirring. Concentrations in mixed lipid vesicles refer to total phospholipid. Also shown is the amplitude of the ThT signal (D) for 5 (▼), 10 (■), and 15 μM (▲) $FtG_{179-194}$ in the presence of increasing concentrations of liposome, recorded at 150 h.

an aldehyde moiety at the end of its truncated *sn*-2 acyl chain, promoted as such as well as in POPC/PoxnoPC liposomes ($X_{PoxnoPC}$ = 0.2) fibril formation by $FtG_{179-194}$ evident as enhanced ThT fluorescence (Figure 3). Instead, the structurally similar 1-palmitoyl-2-azelaoyl-*sn*-glycero-3-phosphocholine (PazePC) containing a carboxylic moiety was not efficient in promoting amyloid formation (Figure S2 of the Supporting Information). Notably, under these conditions, there was no significant increase in ThT emission for $FtG_{179-194}$ in the absence of salt (data not shown). This requirement of saline reveals electrostatic screening to be essential for fibril formation by $FtG_{179-194}$ on zwitterionic phospholipid surfaces, allowing proximity, aggregation, and proper alignment of $FtG_{179-194}$ bearing several charges.

In the presence of the POPC/PoxnoPC liposomes ($X_{PoxnoPC}$ = 0.2), the ThT fluorescence increase for $FtG_{179-194}$ showed sigmoidal kinetics (Figure 3). The initial lag phase can be attributed to a nucleation preceding a relatively fast fibril elongation−growth phase. It is possible that the first event in the pathway toward amyloid is dimer formation, which is inherently slow.[41] The reactions were further recorded at varying PoxnoPC/POPC ($X_{PoxnoPC}$ = 0.2) liposome and $FtG_{179-194}$ concentrations. The enhancement of ThT intensity was ~4-fold when the concentration of $FtG_{179-194}$ was doubled to 10 μM. The final ThT fluorescence intensity levels after the completion of fibrillation increased with the total lipid concentration (Figure 3D). However, there was an only slight variation in the lag time as a function of lipid concentration (Figure 3).

We then followed the fibrillation kinetics for $FtG_{179-194}$ by ThT fluorescence over a period of up to 240 h in the presence of varying concentrations of PoxnoPC as such, both below and above the critical micelle concentration (CMC) of 22.5 μM determined for this lipid.[42] A small immediate increase in fluorescence was followed by a much larger sigmoidal increase in emission with time (Figure 4). Kinetic parameters (lag time, $t_{1/2}$, and K_{app}) were derived for each of these curves by fitting the data as described in Materials and Methods. All kinetic curves in the presence of PoxnoPC were consistent with nucleation-dependent kinetics.[36]

The ThT fluorescence for $FtG_{179-194}$ was enhanced several-fold in the presence of PoxnoPC both below and above the CMC. Increasing the peptide concentration from 5 to 15 μM augmented the amplitude of ThT emission linearly with a PoxnoPC concentration below the CMC (Figure 5A), reaching a plateau at ~25−30 μM lipid and then decreasing at higher lipid concentrations (Figure 6A). For 20 μM $FtG_{179-194}$, however, the maximal

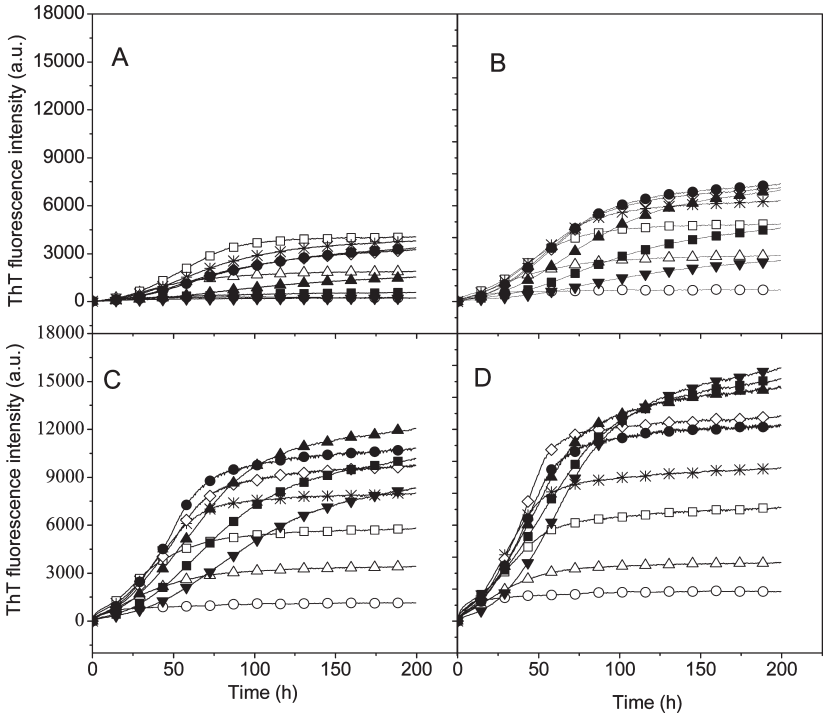

Figure 4. Influence of PoxnoPC on fibril formation by $FtG_{179-194}$ monitored by ThT fluorescence. Kinetics of fibril formation by 5 (A), 10 (B), 15 (C), and 20 μM (D) peptide in the presence of 0 (○), 6.25 (△), 12.5 (□), 20 (∗), 25 (◇), 30 (●), 50 (▲), 75 (■), and 100 μM (▼) PoxnoPC in a total volume of 200 μL of 50 μM ThT in 20 mM Hepes, 0.1 mM EDTA, and 150 mM NaCl (pH 7.0). Fluorescence was measured at 27 °C without agitation or stirring of the covered contents.

intensity or amplitude increased even at >30 μM PoxnoPC, yet at a different rate (Figure 6A). Above the CMC, the emission intensity of ThT increased sharply with an increase in the peptide concentration with reciprocal changes in the lag time and $t_{1/2}$ (panels A−C, respectively, of Figure 5). Under these conditions, the rate K_{app} of $FtG_{179-194}$ amyloid formation increased with PoxnoPC concentration, approached a maximum around 25 μM lipid, and then decreased above 30 μM PoxnoPC (Figure 6D). PoxnoPC at close to micellar concentrations (~22.5 μM) induced a maximal increase in ThT fluorescence as compared to either below or above the CMC. Above the CMC (>25−30 μM), an increasing PoxnoPC concentration decreased progressively the value of K_{app} for fibril formation (Figure 6D), most likely reflecting surface dilution of the peptide. The opposite, an increase in K_{app}, was observed with an increase in peptide concentration above the CMC (Figure 5D). However, the increase in the rate of fibrillation was significantly smaller than that below the CMC.

The half-lives ($t_{1/2}$) of the reactions increased with PoxnoPC concentration both below and above the CMC and were for most cases longer than those recorded for the peptide alone at the same concentration. The amplitude of ThT fluorescence enhancement and lag time were proportional to the PoxnoPC concentration, while the lag time showed a biphasic relationship. Prolonging the lag time and $t_{1/2}$ suggests that PoxnoPC decreased the rates of nucleation and fibril elongation.

Trp Fluorescence Spectroscopy of $FtG_{179-194}$. The sensitivity of Trp fluorescence to the environment is used to monitor the interaction of $FtG_{179-194}$ with lipids. W180 in $FtG_{179-194}$ in buffer has an emission maximum at 352 nm (data not shown), typical for an aqueous environment.[43] In the presence of POPC/PoxnoPC (X = 0.2) liposomes, the emission intensity was slightly attenuated without other effects on the spectra. The reduction in the quantum yield of W180 in POPC/PoxnoPC (X = 0.2) liposomes is likely to result from this residue contacting the membrane hydrocarbon−water interface, moving into the proximity of the charges of the P^{-}-N^{+} dipole of the phosphocholine headgroup, allowing π-orbital−cation interaction.[44] In contrast, upon addition of neat PoxnoPC, the emission intensity was progressively enhanced as a function of the lipid:peptide molar ratio, reaching a plateau close to a 1:1 $FtG_{179-194}$:PoxnoPC molar ratio (Figure 7A), suggesting that $FtG_{179-194}$ forms a stoichiometric complex with this oxidatively modified phospholipid.

The observed increase in W180 emission upon the binding of $FtG_{179-194}$ to PoxnoPC suggests a direct interaction of W180 with a hydrophobic part of PoxnoPC. To investigate the orientation of $FtG_{179-194}$ in the membrane surface, we used the neutral water-soluble collisional quencher acrylamide. Stern−Volmer plots, recorded in the absence and presence of PoxnoPC, show the fluorescence of W180 decreases in a concentration-dependent manner upon addition of acrylamide in the absence and presence of PoxnoPC (Figure 7B), without other effects on the spectra (data not shown). Compared with the measurements in the absence of lipid, the values for K_{sv} decreased in the presence of PoxnoPC (Table 1), while in the presence of 50 μM PoxnoPC (i.e., above the CMC), a considerably diminished quenching was evident, thus revealing W180 becomes less accessible to acrylamide. The value for K_{sv} above the CMC of PoxnoPC is lower than the value measured below the CMC, thus suggesting a partial shielding of W180 from contacts with the aqueous phase in PoxnoPC micelles, in keeping with the observed elevated quantum yield (Figure 7A).

The changes in W180 fluorescence described above become evident within approximately 1 min of the mixing of $FtG_{179-194}$

dx.doi.org/10.1021/bi200195s |*Biochemistry* 2011, 50, 4877–4889

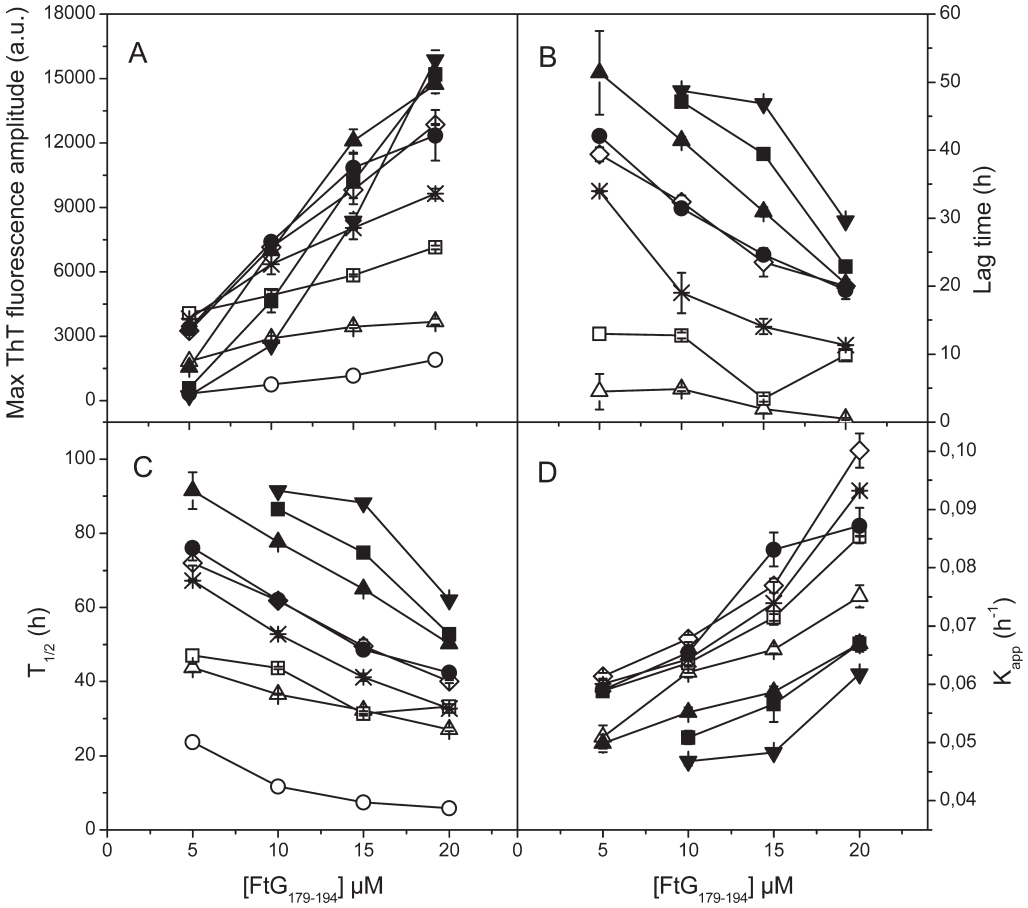

Figure 5. Amplitude of ThT emission (A), lag time (B), $t_{1/2}$ (C), and K_{app} [apparent growth rate constant (D)] for 0 (○), 6.25 (△), 12.5 (□), 20 (∗), 25 (◇), 30 (●), 50 (▲), 75 (■), and 100 μM (▼) PoxnoPC in the presence of varying concentrations of FtG$_{179-194}$. Each point represents the average of three independent experiments with the error bars representing their standard deviation and the solid lines interconnecting each derived data point.

and these lipids. Subsequently, we studied possible longer-term effects of PoxnoPC on the Trp fluorescence of this peptide as a function of time. A pronounced and progressive enhancement of W180 emission was observed in the course of the initial 6 h of interaction (Figure 8A), suggesting that W180 in FtG$_{179-194}$ is being transferred into a hydrophobic milieu, as also indicated by a minor blue shift in the Trp emission spectra (Figure 8A). After this increase, the fluorescence intensity then declines, without affecting the wavelength maximum of Trp emission.

These changes in W180 fluorescence were monitored with continuous stirring, and the kinetics are therefore not comparable to the ThT fluorescence data shown above, measured without stirring. To correlate the time dependence of the changes in W180 and ThT fluorescence, we also measured data for the latter dye with stirring (Figure 8B). Under these conditions, the increase in ThT emission reaches a maximum within approximately 4 h. It is possible that ThT as such enhances the rate of fibril formation, as suggested for the other amyloid staining dye, Congo Red.[45] Along these lines, the increase in λ_{max} for ThT is even faster, being completed in approximately 3 h (Figure 8B). This time range also correlated with the differential fluorescence change measured for W180 in the presence of acrylamide (Figure 8C), these data demonstrating the fluorophore becoming progressively more exposed to the quencher during the growth of the amyloid fibril. The latter could suggest that the growing fibril is being transferred into the aqueous phase from the lipid−water interface nucleating fibril growth.

To conclude, our data from Trp and ThT spectroscopy suggest several consecutive processes, as follows. First, there is a rapid (within 1 min) interaction between PoxnoPC and FtG$_{179-194}$, resulting in an increase in W180 emission, together with a minor decrease in λ_{max} (blue shift). Simultaneously, the access of acrylamide to W180 is reduced, suggesting that the peptide could enter into the membrane or reside at the level of the PC headgroup, while the extended conformation adapted by the oxononanoyl chain would be shielding the Trp from the quencher. This change in Trp180 fluorescence reaches a maximum in approximately 6−8 h, coinciding with the time required to reach a maximum in ThT emission (approximately 6 h), while the change in the λ_{max} for ThT fluorescence reached a plateau within approximately 3 h. This first phase is likely to report on the aggregation and formation of amyloid fibril structure induced by PoxnoPC.

The next phase (after ≈6 h) is revealed by the progressive decrease in Trp emission, observed after the peak in fluorescence intensity. The detailed molecular events could not be deciphered at this time. One possibility is a slow structural transition and assembly of the fibrils into amyloid fibrils, suggested by electron microscopy (see below).

FtG$_{179-194}$ Fibrillation Observed by Transmission Electron Microscopy (TEM). TEM of the FtG$_{179-194}$ aggregates formed by the peptide alone or in the presence of PoxnoPC revealed a large network of long fibrils (Figures 9 and 10) with different morphologies (branched, straight, and curved), with

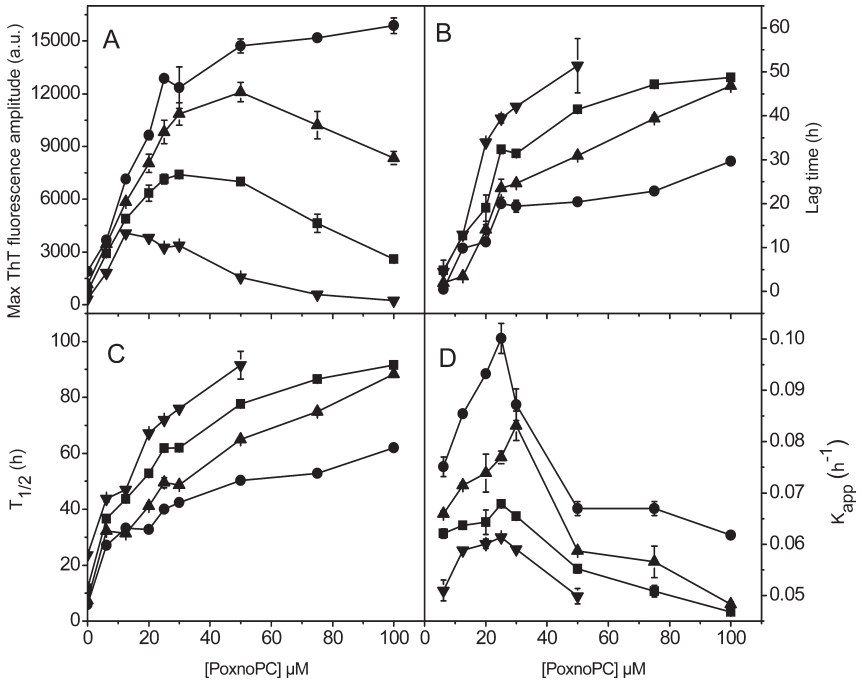

Figure 6. Amplitude of ThT emission (A), lag time (B), $t_{1/2}$ (C), and K_{app} [apparent growth rate constant (D)] for 5 (▼), 10 (■), 15 (▲), and 20 μM (●) $FtG_{179-194}$ in the presence of varying concentrations of PoxnoPC. $t_{1/2}$, the time required to reach 50% of the maximal fluorescence, was determined from normalized ThT fluorescence intensity data in Figure 2. The K_{app} and lag time were determined by fitting the data in Figure 2 with a logistic sigmoidal curve (eq 1) and plotted vs PoxnoPC concentration. Each point represents the average of three independent experiments with the error bars representing their standard deviation and the solid lines interconnecting each derived data point.

small spherical aggregates observed at early stages of aggregation. We could not observe micelles or vesicles bound to the fibrils. Fibers were of variable length and showed no twisting along the fiber axis. The morphology of amyloid filaments developed with time, presumably upon the establishment of interactions between stable protofilaments, assembled into highly ordered (amyloid fiber) superstructures (Figure 10).

■ DISCUSSION

Oxidative stress, either in the affected lesions such as in the central nervous system during the development of neurodegenerative diseases or in the pancreas developing type 2 diabetes,[46,47] leads to a plethora of chemical modifications of biomolecules, including oxidative scission of polyunsaturated fatty acyl chains.[20] Tissue specific modifications of lipids or lipid profiles could influence the local deposition of amyloid and thus under specific circumstances exacerbate pathological processes.[24,48,49] The oxidation of polyunsaturated phospholipids involves complex chemistry, with a number of short-lived intermediates.[20] The zwitterionic PoxnoPC that was used in this study is derived from abundant phospholipids of human membranes, viz., phosphatidylcholines bearing a *cis*-9 double bond containing fatty acid (e.g., palmitoleic, linoleic, or linolenic acid) at the *sn*-2 position.[20] PoxnoPC has been recognized as the main product of ozone-mediated oxidation of lung surfactant extract, possessing apoptosis and necrosis promoting activity.[50] Here we demonstrate that PoxnoPC efficiently accelerates amyloid fibrillation of $FtG_{179-194}$, whereas $wtG_{179-194}$ was nonamyloidogenic under all conditions studied by us. Human skin is the part of the body most exposed to UV light, which also causes lipid oxidation.[20] This could explain the heavy gelsolin amyloid load in the cutaneous tissue, resulting in cutis laxa in FAF, distinct from other amyloid diseases.[23] It was shown previously that heparin accelerates gelsolin fibrillation at low pH. However, under these conditions, wild-type gelsolin was as amyloidogenic as the mutant D187N fragments,[51,52] yet only the D187N or -Y mutant is involved in gelsolin amyloidosis in FAF.[53] Our results are consistent with the in vivo observations described above as accelerated fibril formation in the presence of PoxnoPC was seen with only $FtG_{179-194}$. Our findings suggest that interactions of the extracellular D187N mutant gelsolin with oxidized phospholipids such as PoxnoPC could be involved and causative in the development of FAF. PoxnoPC is also formed upon oxidation of plasma low-density lipoprotein[54] and is thus predominantly found in the extracellular compartment, which may explain why only secreted mutant gelsolin forms amyloid.[19]

There are no approved therapies for treating amyloid diseases. While many small organic molecules have been reported to inhibit fibrillation in vitro,[55] most of these are either flavonoids or polyphenolic compounds also having antioxidant and anti-inflammatory activities.[56−59] Several lines of reasoning together with a growing number of in vitro results[21,22,30−32] such as those described here converge to suggest that oxidatively modified lipids may be significant in promoting the formation of amyloid plaques in vivo.[24]

Interactions between an amyloid-forming protein and membranes containing oxidized phospholipids are important for two reasons. On one hand, the presence of an oxidized phospholipid accelerates fibrillation,[30−32] and on the other hand, amyloid fibrillation augments oxidative stress further upon the entry of the fibril-forming peptide or protein into cells, obtaining access to mitochondria, thus promoting further formation of oxidized phospholipids and the induction of apoptosis.[24] The formation

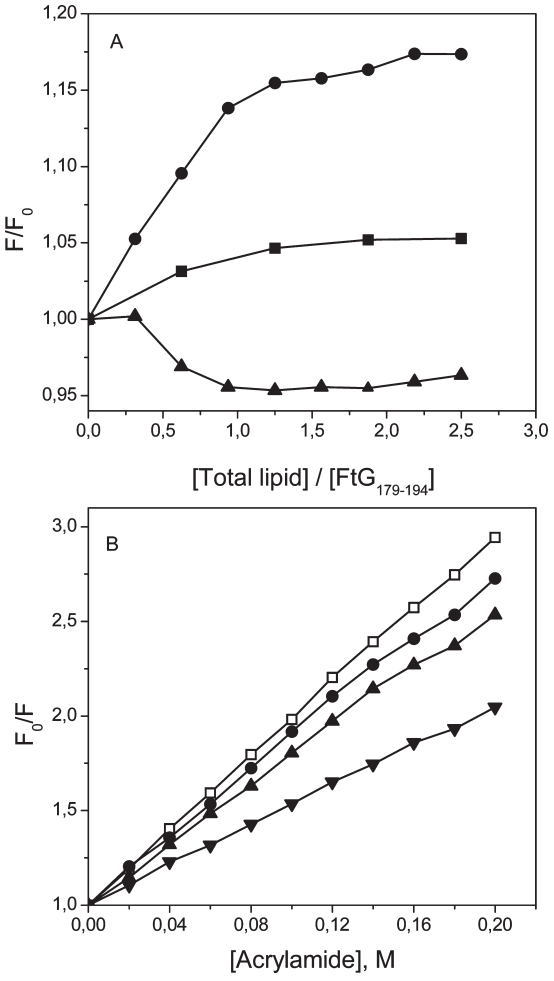

Figure 7. (A) Relative fluorescence intensity of Trp180 for 10 (■) and 20 μM (●) $FtG_{179-194}$ with the data points measured 1 min after each consecutive addition of PoxnoPC as such and depicted as a function of the lipid:peptide molar ratio. Also shown is the decrease in fluorescence seen in the presence of POPC/PoxnoPC [$X_{PoxnoPC}$ = 0.2 (▲)] liposomes. (B) Stern−Volmer plots for the quenching by acrylamide of W180 fluorescence for 20 μM $FtG_{179-194}$ as such in a total volume of 1.8 mL of 20 mM Hepes, 0.1 mM EDTA, and 150 mM NaCl (pH 7.0) (□) and in the presence of 12.5 (■), 25 (▲), and 50 μM (▼) PoxnoPC, i.e., below, at, and above the CMC of this lipid. The temperature was held at 25 °C with a circulating water bath.

of fibers by several amyloid-forming peptides and their cytotoxic action appear to be interconnected, membrane-associated processes,[24,29] with lipid−protein interactions enhancing the rates of peptide aggregation and fibrillogenesis observed in the presence of lipids, for instance, when containing anionic phospholipids, the latter concentrating and aligning the peptide on the membrane surface.[60,61] In contrast to PoxnoPC, the other lipids studied had no effect on $FtG_{179-194}$ fibrillation. The introduction of polar functional groups at the end of the *sn*-2 acyl chain due to oxidation is readily expected to have pronounced effects on the membrane biophysical properties, including the polarity profile and overall lipid organization.[24] More specifically, the oxidatively modified chains no longer remain in the membrane hydrocarbon region but can adopt the so-called extended conformation,[62] protruding into the aqueous phase.[42,63] Accordingly, the constraints due to the hydrophobicity become altered,

Table 1. Stern−Volmer Quenching Constants [K_{sv} (M^{-1})] of Acrylamide for 20 μM $FtG_{179-194}$ in the Absence and Presence of PoxnoPC at the Indicated Concentrations

	buffer	with 12.5 μM PoxnoPC	with 25 μM PoxnoPC	with 50 μM PoxnoPC
K_{sv}	9.75	8.61	7.76	5.23

with hydrophobic environments extending both out- and inward from the lipid membrane polar headgroup region.

Previously, it has been reported that submicellar concentrations of SDS, alkyl bromide, and the short chain phospholipid dihexanoylphosphatidylcholine accelerate fiber formation by α-synuclein,[64] Alzheimer's β-peptide,[65] and apolipoprotein C-II,[66] respectively, yet fibrillation of these peptides was attenuated above the CMC of the amphiphiles. The CMC of PoxnoPC is ~23 μM,[42] and this lipid promotes $FtG_{179-194}$ fibril formation both below and above the CMC. While the rate of fibril formation by $FtG_{179-194}$ decreased above the CMC of PoxnoPC, the extent of fibrillation was directly dependent on PoxnoPC concentration also above the CMC as observed from the maximum in ThT intensity. Notably, the effects of PoxnoPC on $FtG_{179-194}$ fibril formation below the CMC were clearly different from those of PoxnoPC micelles. The increase in W180 emission upon the addition of PoxnoPC to $FtG_{179-194}$ suggests a stoichiometric reaction, with the formation of a 1:1 complex and a contact of this residue with a hydrophobic region of PoxnoPC. However, efficient quenching by acrylamide reveals W180 below the CMC of PoxnoPC to reside in contact with the aqueous phase, in spite of the minor decrease in environment polarity suggested by the augmented quantum yield. Above the CMC, the increase in Trp emission could result from W180 being accommodated in the hydrocarbon region of the micelle. However, this would be expected to more drastically reduce the value of K_{sv}. Accordingly, it is possible that W180 resides in the interface, in contact with the *sn*-2 oxononanoyl chains of PoxnoPC extending out of the micelle surface.

The apparent first-order rate constant K_{app} of fibril formation increased as the PoxnoPC monomer concentration in solution was increased below the CMC of the lipid, reaching a maximum at CMC and then progressively decreasing above the CMC (Figure 6D). Simultaneously, the lag time was prolonged, with a sigmoidal dependence on lipid concentration. Increasing the $FtG_{179-194}$ concentration promoted fibril formation both below and above the CMC, decreasing the lag and increasing K_{app} and $t_{1/2}$. The latter dependencies suggest that the concentration of reactive species increased with an increasing $FtG_{179-194}$ concentration, revealing that the acceleration of fibrillation is directly dependent on both the concentration and the physical (aggregation) state of PoxnoPC. It is possible that the monomeric lipid acts directly in the peptide aggregation process after formation of the complex with the $FtG_{179-194}$ peptide and then becomes incorporated in some way into the protofilaments prior to their assembly into fibrils. Above the CMC, the number of productive collisions between the reactive peptides is expected to decline due to surface dilution, with a decrease in K_{app} and the maximum yield of fibrils (measured by ThT fluorescence), with a prolongation of lag time and $t_{1/2}$ (Figure 6). The importance of surface dilution above the CMC is further emphasized by the promotion of fibril formation with an increase in $FtG_{179-194}$ concentration. Unfortunately, premicellar aggregates are in general poorly characterized. Nevertheless, our findings do show that

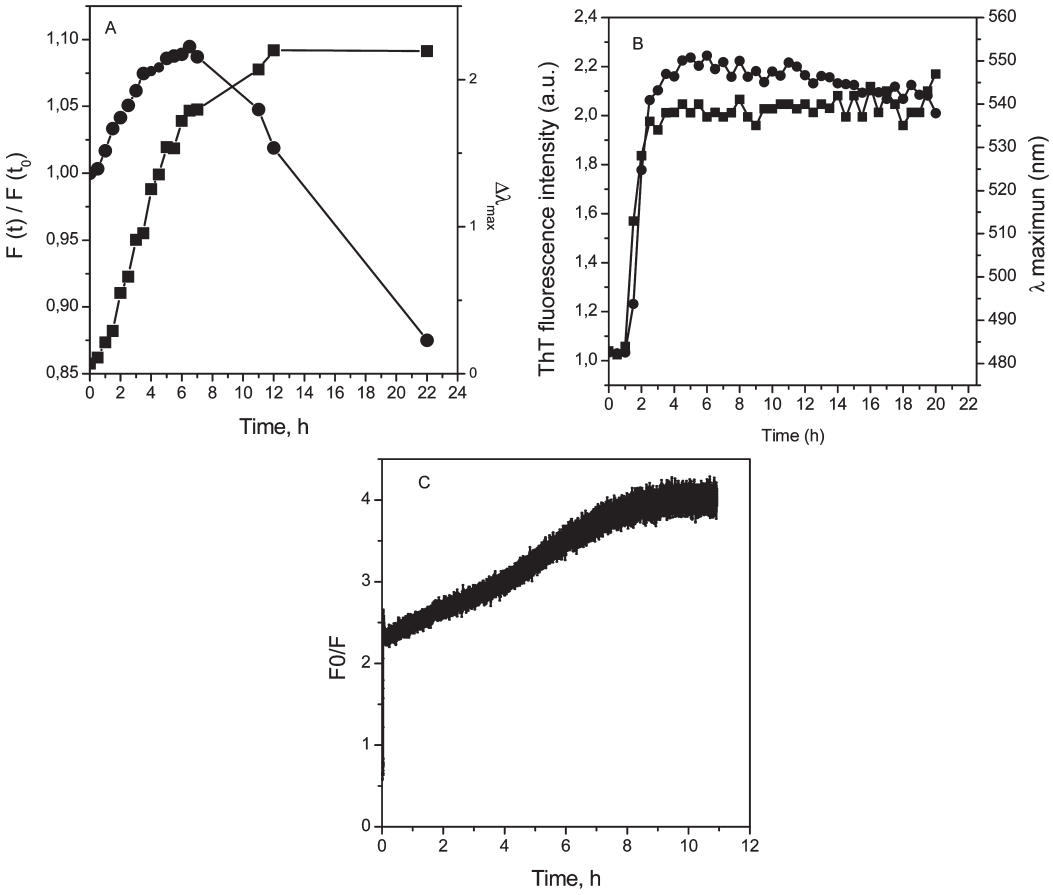

Figure 8. (A) Relative fluorescence intensity (left-hand *Y* axis, ●) and decrease in λ_{max} (blue shift, right-hand *Y* axis, ■) for W180. (B) ThT fluorescence intensity (left-hand *Y* axis, ●) and red shift in ThT emission (right-hand *Y* axis, ■). (C) Time dependence of the quenching of W180 fluorescence by acrylamide for 20 μM $FtG_{179-194}$ as a function of time in a total volume of 1.8 mL of 20 mM Hepes, 0.1 mM EDTA, and 150 mM NaCl (pH 7.0) in the presence of 50 μM PoxnoPC. F_0 and F represent the fluorescence intensities recorded with continuous stirring in the absence and presence of 250 μM acrylamide, respectively. The temperature was kept at 25 °C with a circulating water bath.

oxidized phospholipid-containing membranes play a crucial role in the aggregation process, with PoxnoPC promoting nucleation and amyloid formation by $FtG_{179-194}$ on the membrane surfaces, as well as in solution, reacting with this oxidized phospholipid below its CMC.

Altered Reaction Kinetics in the Presence of PoxnoPC. Our data show that augmented fibril formation by $FtG_{179-194}$ in the presence of PoxnoPC is regulated by a mechanism leading to a stable nucleus as in a simple nucleation-dependent model. The lag time depends on the aggregation state of PoxnoPC, being different below and above the CMC for this lipid. The aldehyde moiety of the *sn*-2 chain appears to be important in promoting protofibril formation, most likely involving a Schiff base. The appearance of a concentration-dependent lag phase preceding fibril formation by $FtG_{179-194}$ suggests a metastable intermediate. It is unclear how PoxnoPC stabilizes the protofibrils. The formation of a transient complex is fast below the CMC, in the presence of premicellar aggregates of PoxnoPC. This is consistent with our data on amyloid formation in the presence of PoxnoPC and is also supported by the finding that phospholipids may convert inert fibrils back to neurotoxic protofibrils[67] and stabilize toxic oligomers.[68] Accordingly, PoxnoPC may stabilize transient protofibrils and prefibrillar structures in the folding–aggregation free energy landscape preceding the formation of a nontoxic mature amyloid,[24] similarly to that recently suggested for the functional amyloid formation acting as an on–off switch controlling the activity of phospholipase A2.[28]

Two distinct lines of evidence lend support to the view described above. First, the lag time of fibril formation increases with PoxnoPC concentration below the CMC (Figure 6C), suggesting that steps preceding the formation of a nucleus are significant to the reaction. Below the CMC, the lag time is rather independent of peptide concentration (Figure 5B). Second, in the presence of acrylamide, three different rates of quenching of W180 were observed during fibril formation (Figure 8B). W180 fluorescence data suggest a the formation of a 1:1 complex by PoxnoPC and $FtG_{179-194}$ (Figure 7A). Below the CMC of PoxnoPC, the coupling of PoxnoPC (most likely via a Schiff base) could involve more diverse NH_2 groups of $FtG_{179-194}$, making these peptides amphiphilic and aligning them in different orientations (Figure 11). Typical amino acids reacting with aldehydes are lysine, arginine, Figure 11histidine, and cysteine, which are not present in $FtG_{179-194}$. The moiety in $FtG_{179-194}$ reacting with PoxnoPC thus remains unclear. The amyloid-forming core sequence in $FtG_{179-194}$ is assigned to residues CNFIL. The formation of parallel β-sheet structure appears unlikely as this would require Asp191 residues in adjuscent polypeptide chains to be in the proximity. Accordingly, it seems feasible that the $FtG_{179-194}$ fibrils are antiparallel.[69]The kinetics become attenuated by the initial heterogeneity of the reaction

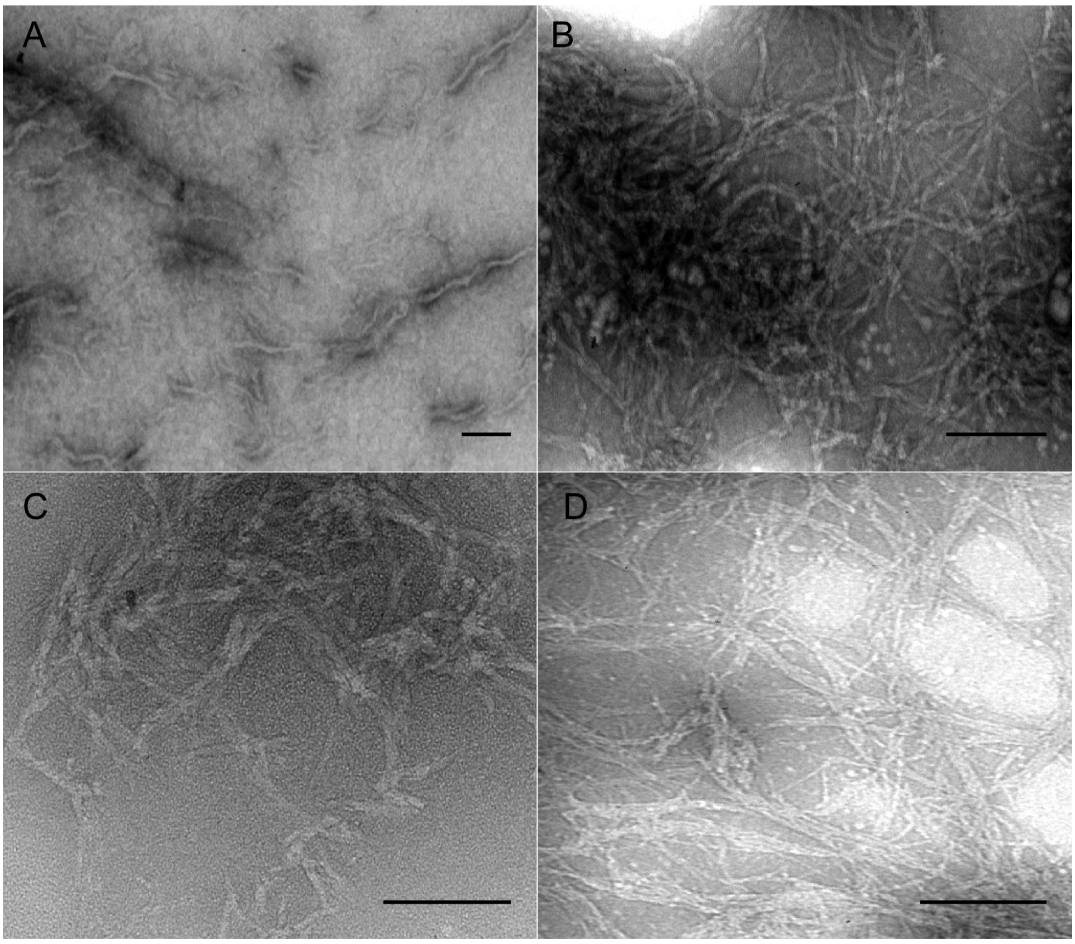

Figure 9. Transmission electron micrographs of fibrils formed by 15 μM $FtG_{179-194}$ as such (A) and in the presence of 12.5 (B), 25 (C), and 50 μM (D) PoxnoPC, upon incubation for 90−100 h. Scale bars represent 200 nm.

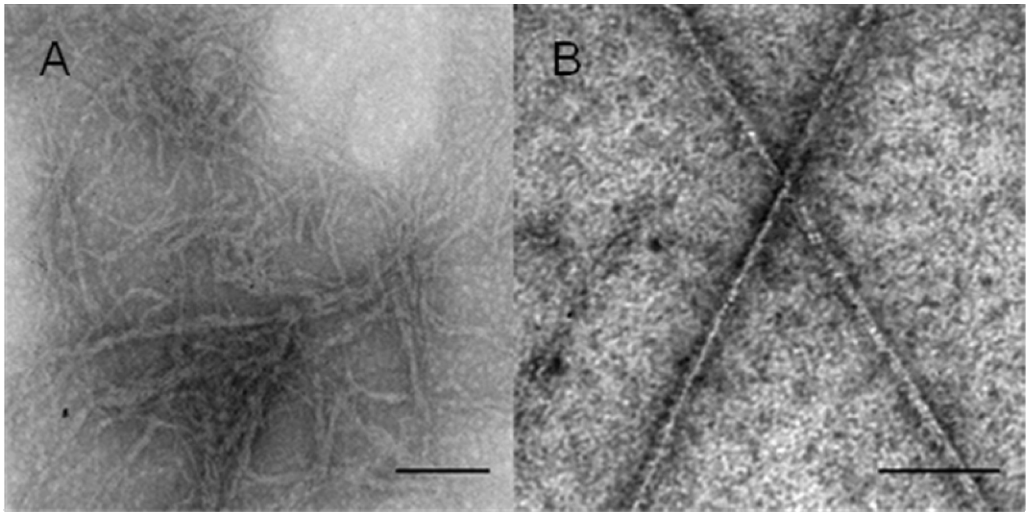

Figure 10. Transmission electron micrographs of fibrils formed by 10 μM $FtG_{179-194}$ in the presence of 10 μM PoxnoPC after 66 (A) and 160 h (B). Scale bars represent 200 nm.

products of PoxnoPC and the peptide. Notably, Schiff bases are thermally unstable,[70] and subsequent slow conversion could involve restructuring and realignment of the fibrils. This rearrangement could occur during the alignment of aggregated fibrils into linear more macroscopic bundles such as seen by EM (Figure 10B).

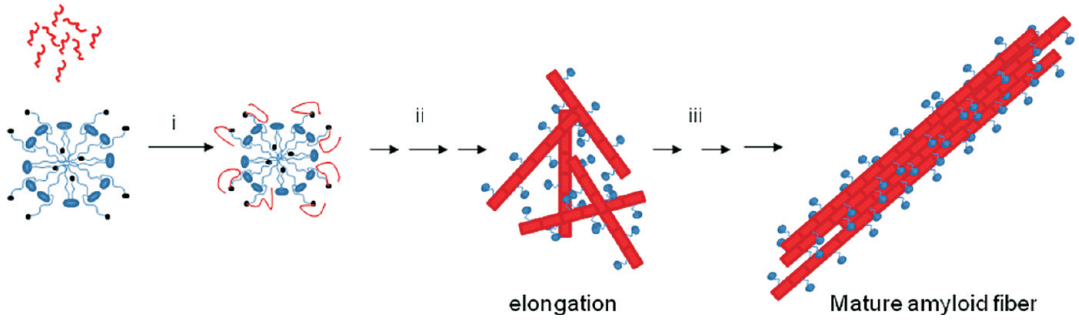

Figure 11. Schematic model for formation of fibrils by $FtG_{179-194}$ in the presence of a PoxnoPC micelle, obeying the concentration-dependent nucleation mechanism. See the text for details.

The ThT intensity profiles above the CMC suggest that the nucleation from the transient lipid−peptide intermediates is slow and rate-limiting with respect to the overall fibril formation process. The time required for nucleation appears as the lag phase, which is dependent on PoxnoPC concentration, with an increasing PoxnoPC concentration increasing the number of intermediate species that can associate to form a nucleus. It seems feasible that the increase in Trp180 fluorescence observed on a time scale before the enhancement of ThT emission reflects the nucleation phase, i.e., the first event in amyloid fiber assembly. This stage seems to involve the formation of a 1:1 complex by PoxnoPC and $FtG_{179-194}$, most likely involving a Schiff base. Fibril elongation would then proceed via the addition of monomers to the existing nuclei. This mechanism would comply with the lack of variation in the lag time upon variation of the concentration of PoxnoPC containing liposomes. The faster aggregation kinetics with an increasing liposomes concentration at a particular peptide concentration would be a consequence of the higher effective concentration of the peptide in the lipid bilayer relative to the bulk.

A detailed understanding of the mechanisms underlying amyloid formation in FAF is important in its own right. Moreover, gelsolin has been observed to be able to attenuate and reverse amyloid formation by the Alzheimer's β-peptide.[71] This finding provides another significant reason to explore gelsolin aggregation and its ability to form amyloid, particularly in light of gelsolin being able to suppress neurotoxicity in Alzheimer's disease animal models.[72]

■ ASSOCIATED CONTENT

Supporting Information. Lack of ThT fluorescence enhancement for $wtG_{179-194}$ in the presence of only PoxnoPC or with POPC/PoxnoPC ($X_{PoxnoPC}$ = 0.2) liposomes (Figure S1) and structurally similar PazePC containing a carboxylic moiety that was not efficient in promoting the amyloid formation as such or with POPC/PazePC (X_{PazePC} = 0.2) liposomes (Figure S2). This material is available free of charge via the Internet at http://pubs.acs.org.

■ AUTHOR INFORMATION

Corresponding Author

*Helsinki Biophysics and Biomembrane Group, Department of Biomedical Engineering and Computational Science, P.O. Box 12200 (Rakentajanaukio 3), FIN-00076 Aalto, Finland. Phone: +358 50 540 4600. Fax: +358 9 470 23182. E-mail: paavo.kinnunen@aalto.fi.

Funding Sources

This study was supported by the Sigrid Jusélius Foundation, European Science Foundation EuroMEMBRANE CRP OXPL, and the Finnish Academy.

■ ACKNOWLEDGMENT

We thank Kristiina Söderholm for technical assistance and Juha-Matti Alakoskela and Vladimir Zamotin for helpful discussions. A.K.M. additionally thanks J.-P. Mattila for discussions in the early phases of this study and bringing ref 36 to his attention.

■ ABBREVIATIONS

CMC, critical micelle concentration; EDTA, ethylenediaminetetraacetic acid; FAF, Finnish type familial amyloidosis; FtG, Finnish mutant type D187N gelsolin; $FtG_{179-194}$, fragment of FtG residues 179−194; Hepes, *N*-(2-hydroxyethyl)piperazine-*N*′-2-ethanesulfonic acid; K_{app}, apparent rate constant; LUV, large unilamellar vesicle; MMP, matrix metalloprotease type 1; PazePC, 1-palmitoyl-2-azelaoyl-*sn*-glycero-3-phosphocholine; POPC, 1-palmitoyl-2-oleoyl-*sn*-glycero-3-phosphocholine; POPG, 1-palmitoyl-2-oleoyl-*sn*-glycero-3-phospho-*rac*-glycerol; PoxnoPC, 1-palmitoyl-2-(9′-oxononanoyl)-*sn*-glycero-3-phosphocholine; ROS, reactive oxygen species; SDS, sodium dodecyl sulfate; *sn*, stereochemical notation; $t_{1/2}$, time to reach 50% of the maximal fluorescence; ThT, thioflavin T; UV, ultraviolet; wt, wild type; wtG, wild type gelsolin; $wtG_{179-194}$, wild type gelsolin peptide 179−194; X, mole fraction.

■ REFERENCES

(1) de la Chapelle, A., Kere, J., Sack, G. H., Jr., Tolvanen, R., and Maury, C. P. (1992) Familial Amyloidosis, Finnish Type: G654 → A Mutation of the Gelsolin Gene in Finnish Families and an Unrelated American Family. *Genomics 13*, 898–901.

(2) Ikeda, M., Mizushima, K., Fujita, Y., Watanabe, M., Sasaki, A., Makioka, K., Enoki, M., Nakamura, M., Otani, T., Takatama, M., and Okamoto, K. (2007) Familial Amyloid Polyneuropathy (Finnish Type) in a Japanese Family: Clinical Features and Immunocytochemical Studies. *J. Neurol. Sci. 252*, 4–8.

(3) Maury, C. P., Kere, J., Tolvanen, R., and de la Chapelle, A. (1992) Homozygosity for the Asn187 Gelsolin Mutation in Finnish-Type Familial Amyloidosis is Associated with Severe Renal Disease. *Genomics 13*, 902–903.

(4) Kiuru, S., Nieminen, T., and Partinen, M. (1999) Obstructive Sleep Apnoea Syndrome in Hereditary Gelsolin-Related Amyloidosis. *J. Sleep Res. 8*, 143–149.

(5) Kiuru-Enari, S., Keski-Oja, J., and Haltia, M. (2005) Cutis Laxa in Hereditary Gelsolin Amyloidosis. *Br. J. Dermatol. 152*, 250–257.

(6) Tanskanen, M., Paetau, A., Salonen, O., Salmi, T., Lamminen, A., Lindsberg, P., Somer, H., and Kiuru-Enari, S. (2007) Severe Ataxia with Neuropathy in Hereditary Gelsolin Amyloidosis: A Case Report. *Amyloid 14*, 89–95.

(7) Shokouhi, G., and Khosroshahi, H. T. (2008) Ardalan-Shoja-Kiuru Syndrome: Hereditary Gelsolin Amyloidosis Plus Retinitis Pigmentosa. *Nephrol., Dial., Transplant. 23*, 1071, author reply 1071−1072.

(8) Maury, C. P. (1991) Gelsolin-Related Amyloidosis. Identification of the Amyloid Protein in Finnish Hereditary Amyloidosis as a Fragment of Variant Gelsolin. *J. Clin. Invest. 87*, 1195–1199.

(9) Maury, C. P., Kere, J., Tolvanen, R., and de la Chapelle, A. (1990) Finnish Hereditary Amyloidosis is Caused by a Single Nucleotide Substitution in the Gelsolin Gene. *FEBS Lett. 276*, 75–77.

(10) Li, G. H., Arora, P. D., Chen, Y., McCulloch, C. A., and Liu, P. (2010) Multifunctional Roles of Gelsolin in Health and Diseases. *Med. Res. Rev.*.

(11) Burtnick, L. D., Koepf, E. K., Grimes, J., Jones, E. Y., Stuart, D. I., McLaughlin, P. J., and Robinson, R. C. (1997) The Crystal Structure of Plasma Gelsolin: Implications for Actin Severing, Capping, and Nucleation. *Cell 90*, 661–670.

(12) Yin, H. L. (1987) Gelsolin: Calcium- and Polyphosphoinositide-Regulated Actin-Modulating Protein. *BioEssays 7*, 176–179.

(13) Janmey, P. A., and Stossel, T. P. (1987) Modulation of Gelsolin Function by Phosphatidylinositol 4,5-Bisphosphate. *Nature 325*, 362–364.

(14) Kwiatkowski, D. J., Stossel, T. P., Orkin, S. H., Mole, J. E., Colten, H. R., and Yin, H. L. (1986) Plasma and Cytoplasmic Gelsolins are Encoded by a Single Gene and Contain a Duplicated Actin-Binding Domain. *Nature 323*, 455–458.

(15) Lee, W. M., and Galbraith, R. M. (1992) The Extracellular Actin-Scavenger System and Actin Toxicity. *N. Engl. J. Med. 326*, 1335–1341.

(16) Chen, C. D., Huff, M. E., Matteson, J., Page, L., Phillips, R., Kelly, J. W., and Balch, W. E. (2001) Furin Initiates Gelsolin Familial Amyloidosis in the Golgi through a Defect in Ca^{2+} Stabilization. *EMBO J. 20*, 6277–6287.

(17) Huff, M. E., Page, L. J., Balch, W. E., and Kelly, J. W. (2003) Gelsolin Domain 2 Ca^{2+} Affinity Determines Susceptibility to Furin Proteolysis and Familial Amyloidosis of Finnish Type. *J. Mol. Biol. 334*, 119–127.

(18) Blake, C., and Serpell, L. (1996) Synchrotron X-ray Studies Suggest that the Core of the Transthyretin Amyloid Fibril is a Continuous β-Sheet Helix. *Structure 4*, 989–998.

(19) Kangas, H., Seidah, N. G., and Paunio, T. (2002) Role of Proprotein Convertases in the Pathogenic Processing of the Amyloidosis-Associated Form of Secretory Gelsolin. *Amyloid 9*, 83–87.

(20) Fruhwirth, G. O., Loidl, A., and Hermetter, A. (2007) Oxidized Phospholipids: From Molecular Properties to Disease. *Biochim. Biophys. Acta 1772*, 718–736.

(21) Halliwell, B. (1989) Oxidants and the Central Nervous System: Some Fundamental Questions. Is Oxidant Damage Relevant to Parkinson's Disease, Alzheimer's Disease, Traumatic Injury or Stroke?. *Acta Neurol. Scand.* (Suppl. 126), 23–33.

(22) Bieschke, J., Zhang, Q., Bosco, D. A., Lerner, R. A., Powers, E. T., Wentworth, P., Jr., and Kelly, J. W. (2006) Small Molecule Oxidation Products Trigger Disease-Associated Protein Misfolding. *Acc. Chem. Res. 39*, 611–619.

(23) Tanskanen, M., Kiuru-Enari, S., Tienari, P., Polvikoski, T., Verkkoniemi, A., Rastas, S., Sulkava, R., and Paetau, A. (2006) Senile Systemic Amyloidosis, Cerebral Amyloid Angiopathy, and Dementia in a very Old Finnish Population. *Amyloid 13*, 164–169.

(24) Kinnunen, P. K. J. (2009) Amyloid Formation on Lipid Membrane Surfaces. *Open Biol. J. 2*, 163–175.

(25) Esterbauer, H., Schaur, R. J., and Zollner, H. (1991) Chemistry and Biochemistry of 4-Hydroxynonenal, Malonaldehyde and Related Aldehydes. *Free Radical Biol. Med. 11*, 81–128.

(26) Chen, K., Maley, J., and Yu, P. H. (2006) Potential Inplications of Endogenous Aldehydes in β-Amyloid Misfolding, Oligomerization and Fibrillogenesis. *J. Neurochem. 99*, 1413–1424.

(27) Mattila, J. P., Sabatini, K., and Kinnunen, P. K. J. (2008) Oxidized Phospholipids as Potential Molecular Targets for Antimicrobial Peptides. *Biochim. Biophys. Acta 1778*, 2041–2050.

(28) Code, C., Mahalka, A. K., Bry, K., and Kinnunen, P. K. J. (2010) Activation of Phospholipase A2 by 1-Palmitoyl-2-(9′-Oxo-Nonanoyl)-Sn-Glycero-3-Phosphocholine in Vitro. *Biochim. Biophys. Acta 1798*, 1593–1600.

(29) Gorbenko, G. P., and Kinnunen, P. K. J. (2006) The Role of Lipid-Protein Interactions in Amyloid-Type Protein Fibril Formation. *Chem. Phys. Lipids 141*, 72–82.

(30) Komatsu, H., Liu, L., Murray, I. V., and Axelsen, P. H. (2007) A Mechanistic Link between Oxidative Stress and Membrane Mediated Amyloidogenesis Revealed by Infrared Spectroscopy. *Biochim. Biophys. Acta 1768*, 1913–1922.

(31) Koppaka, V., and Axelsen, P. H. (2000) Accelerated Accumulation of Amyloid β Proteins on Oxidatively Damaged Lipid Membranes. *Biochemistry 39*, 10011–10016.

(32) Kinnunen, P. K. J., Domanov, Y. A., Mattila, J. P., and Varis, T. (2011) Formation of Lipid/Peptide Tubules by IAPP and Temporin B on Supported Lipid Membranes. *Soft Matter*10.1039/B925228B.

(33) Maury, C. P., Nurmiaho-Lassila, E. L., and Rossi, H. (1994) Amyloid Fibril Formation in Gelsolin-Derived Amyloidosis. Definition of the Amyloidogenic Region and Evidence of Accelerated Amyloid Formation of Mutant Asn-187 and Tyr-187 Gelsolin Peptides. *Lab. Invest. 70*, 558–564.

(34) Khurana, R., Coleman, C., Ionescu-Zanetti, C., Carter, S. A., Krishna, V., Grover, R. K., Roy, R., and Singh, S. (2005) Mechanism of Thioflavin T Binding to Amyloid Fibrils. *J. Struct. Biol. 151*, 229–238.

(35) Zhao, H., Mattila, J. P., Holopainen, J. M., and Kinnunen, P. K. J. (2001) Comparison of the Membrane Association of Two Antimicrobial Peptides, Magainin 2 and Indolicidin. *Biophys. J. 81*, 2979–2991.

(36) Nielsen, L., Khurana, R., Coats, A., Frokjaer, S., Brange, J., Vyas, S., Uversky, V. N., and Fink, A. L. (2001) Effect of Environmental Factors on the Kinetics of Insulin Fibril Formation: Elucidation of the Molecular Mechanism. *Biochemistry 40*, 6036–6046.

(37) Zhao, H., and Kinnunen, P. K. J. (2002) Binding of the Antimicrobial Peptide Temporin L to Liposomes Assessed by Trp Fluorescence. *J. Biol. Chem. 277*, 25170–25177.

(38) Tallmadge, D. H., Huebner, J. S., and Borkman, R. F. (1989) Acrylamide Quenching of Tryptophan Photochemistry and Photophysics. *Photochem. Photobiol. 49*, 381–386.

(39) Eftink, M. R., and Ghiron, C. A. (1976) Fluorescence Quenching of Indole and Model Micelle Systems. *J. Phys. Chem. 80*, 486–493.

(40) Naiki, H., Higuchi, K., Hosokawa, M., and Takeda, T. (1989) Fluorometric Determination of Amyloid Fibrils in Vitro using the Fluorescent Dye, Thioflavin T1. *Anal. Biochem. 177*, 244–249.

(41) Yonezawa, Y., Tanaka, S., Kubota, T., Wakabayashi, K., Yutani, K., and Fujiwara, S. (2002) An Insight into the Pathway of the Amyloid Fibril Formation of Hen Egg White Lysozyme obtained from a Small-Angle X-ray and Neutron Scattering Study. *J. Mol. Biol. 323*, 237–251.

(42) Sabatini, K., Mattila, J. P., Megli, F. M., and Kinnunen, P. K. J. (2006) Characterization of Two Oxidatively Modified Phospholipids in Mixed Monolayers with DPPC. *Biophys. J. 90*, 4488–4499.

(43) Breukink, E., van Kraaij, C., van Dalen, A., Demel, R. A., Siezen, R. J., de Kruijff, B., and Kuipers, O. P. (1998) The Orientation of Nisin in Membranes. *Biochemistry 37*, 8153–8162.

(44) Dougherty, D. A. (1996) Cation-π Interactions in Chemistry and Biology: A New View of Benzene, Phe, Tyr, and Trp. *Science 271*, 163–168.

(45) Kim, Y. S., Randolph, T. W., Manning, M. C., Stevens, F. J., and Carpenter, J. F. (2003) Congo Red Populates Partially Unfolded States of an Amyloidogenic Protein to Enhance Aggregation and Amyloid Fibril Formation. *J. Biol. Chem. 278*, 10842–10850.

(46) Barnham, K. J., Masters, C. L., and Bush, A. I. (2004) Neurodegenerative Diseases and Oxidative Stress. *Nat. Rev. Drug Discovery 3*, 205–214.

(47) Simonian, N. A., and Coyle, J. T. (1996) Oxidative Stress in Neurodegenerative Diseases. *Annu. Rev. Pharmacol. Toxicol. 36*, 83–106.

(48) Bosco, D. A., Fowler, D. M., Zhang, Q., Nieva, J., Powers, E. T., Wentworth, P., Jr., Lerner, R. A., and Kelly, J. W. (2006) Elevated Levels of Oxidized Cholesterol Metabolites in Lewy Body Disease Brains Accelerate α-Synuclein Fibrillization. *Nat. Chem. Biol. 2*, 249–253.

(49) Butterfield, D. A., and Lauderback, C. M. (2002) Lipid Peroxidation and Protein Oxidation in Alzheimer's Disease Brain: Potential Causes and Consequences Involving Amyloid β-Peptide-Associated Free Radical Oxidative Stress. *Free Radical Biol. Med. 32*, 1050–1060.

(50) Uhlson, C., Harrison, K., Allen, C. B., Ahmad, S., White, C. W., and Murphy, R. C. (2002) Oxidized Phospholipids Derived from Ozone-Treated Lung Surfactant Extract Reduce Macrophage and Epithelial Cell Viability. *Chem. Res. Toxicol. 15*, 896–906.

(51) Ratnaswamy, G., Koepf, E., Bekele, H., Yin, H., and Kelly, J. W. (1999) The Amyloidogenicity of Gelsolin is Controlled by Proteolysis and pH. *Chem. Biol. 6*, 293–304.

(52) Suk, J. Y., Zhang, F., Balch, W. E., Linhardt, R. J., and Kelly, J. W. (2006) Heparin Accelerates Gelsolin Amyloidogenesis. *Biochemistry 45*, 2234–2242.

(53) de la Chapelle, A., Tolvanen, R., Boysen, G., Santavy, J., Bleeker-Wagemakers, L., Maury, C. P., and Kere, J. (1992) Gelsolin-Derived Familial Amyloidosis Caused by Asparagine or Tyrosine Substitution for Aspartic Acid at Residue 187. *Nat. Genet. 2*, 157–160.

(54) Palinski, W., Rosenfeld, M. E., Yla-Herttuala, S., Gurtner, G. C., Socher, S. S., Butler, S. W., Parthasarathy, S., Carew, T. E., Steinberg, D., and Witztum, J. L. (1989) Low Density Lipoprotein Undergoes Oxidative Modification in Vivo. *Proc. Natl. Acad. Sci. U.S.A. 86*, 1372–1376.

(55) Feng, B. Y., Toyama, B. H., Wille, H., Colby, D. W., Collins, S. R., May, B. C., Prusiner, S. B., Weissman, J., and Shoichet, B. K. (2008) Small-Molecule Aggregates Inhibit Amyloid Polymerization. *Nat. Chem. Biol. 4*, 197–199.

(56) Ono, K., Yoshiike, Y., Takashima, A., Hasegawa, K., Naiki, H., and Yamada, M. (2003) Potent Anti-Amyloidogenic and Fibril-Destabilizing Effects of Polyphenols in Vitro: Implications for the Prevention and Therapeutics of Alzheimer's Disease. *J. Neurochem. 87*, 172–181.

(57) Zhu, M., Rajamani, S., Kaylor, J., Han, S., Zhou, F., and Fink, A. L. (2004) The Flavonoid Baicalein Inhibits Fibrillation of α-Synuclein and Disaggregates Existing Fibrils. *J. Biol. Chem. 279*, 26846–26857.

(58) Yang, F., Lim, G. P., Begum, A. N., Ubeda, O. J., Simmons, M. R., Ambegaokar, S. S., Chen, P. P., Kayed, R., Glabe, C. G., Frautschy, S. A., and Cole, G. M. (2005) Curcumin Inhibits Formation of Amyloid β Oligomers and Fibrils, Binds Plaques, and Reduces Amyloid in Vivo. *J. Biol. Chem. 280*, 5892–5901.

(59) Necula, M., Kayed, R., Milton, S., and Glabe, C. G. (2007) Small Molecule Inhibitors of Aggregation Indicate that Amyloid β Oligomerization and Fibrillization Pathways are Independent and Distinct. *J. Biol. Chem. 282*, 10311–10324.

(60) Mahalka, A. K., and Kinnunen, P. K. J. (2009) Binding of Amphipathic α-Helical Antimicrobial Peptides to Lipid Membranes: Lessons from Temporins B and L. *Biochim. Biophys. Acta 1788*, 1600–1609.

(61) Zhao, H., Tuominen, E. K., and Kinnunen, P. K. J. (2004) Formation of Amyloid Fibers Triggered by Phosphatidylserine-Containing Membranes. *Biochemistry 43*, 10302–10307.

(62) Kinnunen, P. K. J. (1992) Fusion of Lipid Bilayers: A Model Involving Mechanistic Connection to HII Phase Forming Lipids. *Chem. Phys. Lipids 63*, 251–258.

(63) Mattila, J. P., Sabatini, K., and Kinnunen, P. K. J. (2008) Interaction of Cytochrome *c* with 1-Palmitoyl-2-azelaoyl-*sn*-glycero-3-phosphocholine: Evidence for Acyl Chain Reversal. *Langmuir 24*, 4157–4160.

(64) Rivers, R. C., Kumita, J. R., Tartaglia, G. G., Dedmon, M. M., Pawar, A., Vendruscolo, M., Dobson, C. M., and Christodoulou, J. (2008) Molecular Determinants of the Aggregation Behavior of α- and β-Synuclein. *Protein Sci. 17*, 887–898.

(65) Sabate, R., and Estelrich, J. (2005) Stimulatory and Inhibitory Effects of Alkyl Bromide Surfactants on β-Amyloid Fibrillogenesis. *Langmuir 21*, 6944–6949.

(66) Hatters, D. M., Lawrence, L. J., and Howlett, G. J. (2001) Sub-Micellar Phospholipid Accelerates Amyloid Formation by Apolipoprotein C-II. *FEBS Lett. 494*, 220–224.

(67) Martins, I. C., Kuperstein, I., Wilkinson, H., Maes, E., Vanbrabant, M., Jonckheere, W., Van Gelder, P., Hartmann, D., D'Hooge, R., De Strooper, B., Schymkowitz, J., and Rousseau, F. (2008) Lipids Revert Inert Aβ Amyloid Fibrils to Neurotoxic Protofibrils that Affect Learning in Mice. *EMBO J. 27*, 224–233.

(68) Johansson, A. S., Garlind, A., Berglind-Dehlin, F., Karlsson, G., Edwards, K., Gellerfors, P., Ekholm-Pettersson, F., Palmblad, J., and Lannfelt, L. (2007) Docosahexaenoic Acid Stabilizes Soluble Amyloid-β Protofibrils and Sustains Amyloid-β-Induced Neurotoxicity in Vitro. *FEBS J. 274*, 990–1000.

(69) Liepina, I., Janmey, P., Czaplewski, C., and Liwo, A. (2004) Towards Gelsolin Amyloid Formation. *Biopolymers 76*, 543–548.

(70) Dudek, G. O., and Dudek, E. P. (1964) Spectroscopic Studies of Keto-Enol Equilibria. VII. Nitrogen-15 Substituted Schiff Bases. *J. Am. Chem. Soc. 86*, 4283–4287.

(71) Ray, I., Chauhan, A., Wegiel, J., and Chauhan, V. P. (2000) Gelsolin Inhibits the Fibrillization of Amyloid β-Protein, and also Defibrillizes its Preformed Fibrils. *Brain Res. 853*, 344–351.

(72) Antequera, D., Vargas, T., Ugalde, C., Spuch, C., Molina, J. A., Ferrer, I., Bermejo-Pareja, F., and Carro, E. (2009) Cytoplasmic Gelsolin Increases Mitochondrial Activity and Reduces Aβ Burden in a Mouse Model of Alzheimer's Disease. *Neurobiol. Dis. 36*, 42–50.